DAO Office Note 1999-03
Document Date October 7, 1999

The Land Surface Component in GEOS: Model Formulation

Robert Atlas, Head
Data Assimilation Office
Goddard Space Flight Center
Greenbelt, Maryland Andrea M. Molod*

Data Assimilation Office, Model Development Group
Goddard Laboratory for Atmospheres

* *General Sciences Corporation,*
a Subsidiary of Science Applications International Corporation, Laurel, Maryland

Goddard Space Flight Center
Greenbelt, Maryland 20771

Abstract

The Goddard Earth Observing System-Terra Data Assimilation System (GEOS-Terra DAS) has been developed by the NASA/Goddard Data Assimilation Office (DAO) to support the Terra launch. The General Circulation Model (GCM) component has undergone substantial development since the use of the GEOS-1 GCM for the DAO multi-year reanalysis. Some major shortcomings of the GEOS-1 system were addressed by coupling the GCM to a fully interactive soil-vegetation-atmospheric-transfer (SVAT) scheme, specifically the MOSAIC land surface model.

The technique used to couple the land surface model to the atmospheric boundary layer was developed in the DAO, and is unique to GEOS-Terra. The DAO technique allows the impact of the surface heterogeneity to be felt throughout the depth of the boundary layer in an attempt to allow the intensity of the turbulence to determine a 'model blending height'. The technique is described here in detail, along with brief descriptions of the land surface model and turbulence parameterization.

Contents

List of Figures

1 Introduction and Rationale

The NASA/Goddard Data Assimilation Office (DAO) has recently developed the Goddard Earth Observing System-Terra Data Assimilation System (GEOS-Terra DAS), the Terra-launch version of the GEOS DAS which will utilize the newly available observations to provide a more realistic estimate of the climate state and the diagnostics of physical processes. The General Circulation Model (GCM) component of the DAS is important because it is largely responsible for providing first-guess fields to the GEOS DAS Physical-space Statistical Analysis System (PSAS) algorithm that are physically consistent with the observations and do not possess unmanageable biases. The GCM must provide these nearly unbiased estimates on a wide variety of temporal scales, ranging from the hourly to the annual or longer. The GCM must also possess enough detailed physical parameterizations to properly interpret and integrate the observational content of PSAS. The need to incorporate the new types of relevant surface or near-surface data that will be available in the EOS era into the assimilation system is essential to the accuracy of any climate assimilation. The ability of the GCM to properly absorb and utilize the analysed ground temperature, for instance, depends on its description of the near-surface physics.

The influence of the physical processes that occur at or near the land surface on the earth's climate have only recently been recognized and characterized. This realization has led to the development and use of SVAT's for GCM's. The exchanges that occur at the land surface interface substantially effect the GCM climate because they act to partition the incoming solar radiation between surface heating, deep soil heating, and sensible and latent heat fluxes, to redistribute the incident precipitation into evaporation, soil storage, groundwater recharge and runoff, and to regulate biogeochemical cycles such as photosynthesis, transpiration and carbon uptake. Some of the climate bias of the GEOS-1 DAS that are associated with errors in the climate of the GEOS-1 GCM (Molod et al., 1996) may very well be due to an inadequate GCM description of land surface processes.

To accomplish the two goals of an accurate GCM climate and the ability to absorb the influence of new data, the DAO model development group has included a fully coupled land surface parameterization scheme (an SVAT, soil-vegetation-atmospheric transfer), among other new parameterizations, in the GEOS-Terra GCM. Coupling the GCM to an interactive land surface model with vegetative controls enhances the ability to properly capture the shortest and longest time scales.

The specific motivations for including an SVAT in the GEOS GCM were to:

- Improve upward fluxes of solar and longwave radiation at the surface
- Improve turbulent heat and moisture fluxes
- Improve clouds and precipitation
- Provide a more accurate representation of the near- surface environment and ground hydrology
- Improve the ability to assimilate near-surface quantities (temperature and moisture)
- Provide the potential for assimilating ground wetness paramenters

- Provide the potential for assimilating snow parameters

The aspects of an SVAT that may provide these improvements are mainly the vegetative controls over evaporation and the additional predictive capability for surface fields. An example of the impact of the predictive capability is the treatment of the soil moisture. The previous version of the GEOS GCM used a specified soil moisture, calculated monthly using observed ground temperature and precipitation from Schemm et al. (1992). The soil moisture was then used, along with a constant, specified ratio of evaporation to potential evapotranspiration, (beta-function) to calculate the latent heat flux. Through the surface energy balance constraint the energy available for sensible heat flux was determined. Such a technique has been used extensively in GCM's until recently, and acts to inhibit any drift in beta or in soil moisture. However, the smaller scale temporal variability cannot be captured, and much of the highly nonlinear feedback between the atmosphere and the land surface is inhibited. The soil surface, for example, cannot respond to an extreme precipitation event by absorbing water, thereby causing errors in the surface energy budget and resultant ground temperature. Even a simple so-called 'bucket' type of land surface model must specify the beta function (usually constant) and cannot properly capture the variety of influences that the atmosphere exerts over surface processes. The impact of the errors in temporal variability on the resultant climate simulation is shown clearly in Koster and Suarez (1994). Betts et al. (1993) demonstrate the impact of an inaccurately simulated diurnal cycle on the climate bias. GEOS-1 and GEOS-2 GCM simulations, and GEOS-1 and GEOS-2 DAS, all show striking errors in the diurnal cycle of ground temperature as compared to station observations, and the diurnal cycle of the ratio of latent to sensible heat flux as compared to FIFE-1987 data.

2 Model Description

2.1 Land-Surface Model

The DAO chose to implement the Koster-Suarez land surface model, known as 'Mosaic', into the GEOS-Terra GCM. This decision was based on the recommendation of the Model Requirements for Data Assimilation at Launch (MRDAL) Panel, a committee assembled by the DAO and made up of modelling experts from the Goddard Lab for Atmospheres and Lab for Hydrospheres.

Mosaic is a Soil-Vegetation- Atmosphere-Transfer model (SVAT) which was developed by Koster and Suarez (1992) based on the Simple Biosphere (SiB) model of Sellers et al (1986). The predicted quantities are deep soil temperature, canopy temperature, three soil moisture layers, a canopy interception reservoir, a canopy air specific humidity, and a snow pack. Mosaic links the physical descriptions of canopy processes with detailed descriptions of soil moisture and temperature transfers, and solves moisture and energy balance equations at each level. The energy and water transfers are modeled using an electrical resistance network analog, where the resistance to the flow of heat or moisture in the ground or to and from the vegetation canopy are functions of specified soil and vegetation parameters. The vegetation canopy essentially determines the surface roughness, which impacts the intensity of turbulence in the canopy and surface layer, controls the surface reflectance through the leaf areal coverage and fraction of live vegetation, and dictates the effective canopy resistance to

the flow of heat or moisture. The sub-grid scale variability of the surface is modeled by viewing each GCM grid cell as a 'mosaic' of independent vegetation stands, using linear aggregation/disaggregation formulae for links to the GCM grid. The vegetation stands, or 'tiles', interact only through the coupling to the GCM atmosphere. The MOSAIC approach to handling sub-grid scale heterogeneities is presented schematically in figure 1, where a sample GCM grid square containing the 'tiles' that describe the mix of surface scene types is shown. In this example, all of the bare soil portions of the grid box are treated as though they are juxtaposed, as are all of the deciduous trees, evergreen trees, and shrubs. Each of these types is assigned a fraction of areal coverage, which is used to compute grid box averaged fluxes by aggregating linearly.

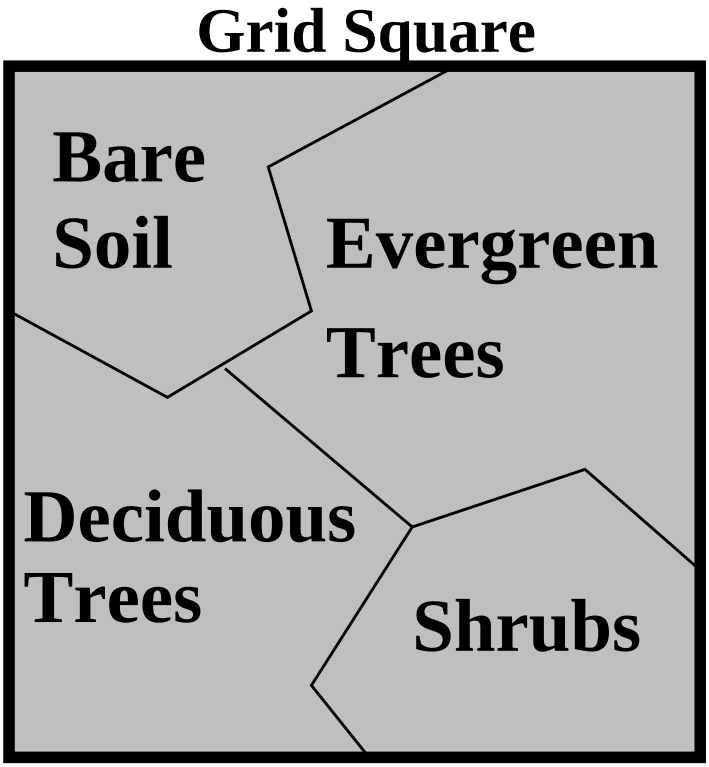

Figure 1: Sample Grid Square Depicting MOSAIC tiles

The Mosaic SVAT in particular offers some features which are particularly suited to the needs of a climate data assimilation system. The computational efficiency, due in part to some approximations and simplifications to the SiB algorithms, makes long assimilations viable. The method of handling sub-grid scale variability, that is, the 'tiles' philosophy, makes possible a reasonable comparison with, and eventual assimilation of, surface station observations of ground temperature. The ability of the GCM to associate the station observations with their particular surface type within a grid cell partly ameliorates the substantial problem of representativeness of highly localized measurements. In addition, the history of Mosaic as an element of the ARIES GCM (Suarez *et al.* 1996),which has many similarities with the GEOS GCM, eased many of the implementation and tuning issues during the process of incorporation into the GEOS-Terra GCM.

2.2 Boundary Layer and Surface Layer over Land

The GEOS GCM turbulence parameterization consists of elements which handle vertical diffusion (Helfand and Labraga, 1988) and surface fluxes of heat, moisture and momentum (Helfand, et al, 1991, and Helfand and Schubert, 1994). The parameterization employs a backward-implicit iterative time scheme. The vertical regime is divided into a free atmosphere, a surface layer, and a viscous sub-layer above the surface roughness elements. The turbulent eddy fluxes are calculated using a variety of methods depending on the vertical location in the atmosphere.

Turbulent eddy fluxes of momentum, heat and moisture in the surface layer are calculated using stability-dependant bulk formulae based on Monin-Obukhov similarity functions. For an unstable surface layer, the chosen stability functions are the KEYPS function (Panofsky, 1973) for momentum, and its generalization for heat and moisture. The function for heat and moisture assures non-vanishing heat and moisture fluxes as the wind speed approaches zero. For a stable surface layer, the stability functions are those of Clarke (1970), slightly modified for the momemtum flux. The moisture flux also depends on a specified evapotranspiration coefficient, dependant on the ground wetness over land. The gradients in the viscous sublayer are based on Yaglom and Kader (1974).

Above the surface layer, turbulent fluxes of momentum, heat and moisture are calculated by the Level 2.5 Mellor-Yamada type closure scheme of Helfand and Labraga (1988), which predicts turbulent kinetic energy and determines the eddy transfer coefficients used for vertical diffusion. The Planetary Boundary Layer (PBL) height is diagnosed by the parameterization as the level at which the turbulent kinetic energy is reduced to a tenth of its surface value.

In the level 2.5 approach, the vertical fluxes of the scalars θ_v, virtual potential temperature, and q, specific humidity, and the wind components u and v are expressed in terms of the diffusion coefficients K_h and K_m, respectively. In the statisically realizable level 2.5 turbulence scheme of Helfand and Labraga (1988), these diffusion coefficients are expressed as

$$K_h = \begin{cases} q\,\ell\,S_H(G_M, G_H) & \text{for decaying turbulence} \\ \frac{q^2}{q_e}\,\ell\,S_H(G_{M_e}, G_{H_e}) & \text{for growing turbulence} \end{cases}$$

and

$$K_m = \begin{cases} q\,\ell\,S_M(G_M, G_H) & \text{for decaying turbulence} \\ \frac{q^2}{q_e}\,\ell\,S_M(G_{M_e}, G_{H_e}) & \text{for growing turbulence} \end{cases}$$

where q here refers to the turbulent kinetic energy, which is half the square of the turbulent fluctuating u-velocity, the subscript e refers to the value under conditions of local equillibrium (obtained from the Level 2.0 Model), ℓ is the master length scale related to the vertical structure of the atmosphere, and S_M and S_H are functions of G_H and G_M, the dimensionless buoyancy and wind shear parameters, respectively. Both G_H and G_M, and their equilibrium values G_{H_e} and G_{M_e}, are functions of the Richardson number:

$$RI = \frac{\frac{g}{\theta_v}\frac{\partial \theta_v}{\partial z}}{(\frac{\partial u}{\partial z})^2 + (\frac{\partial v}{\partial z})^2} = \frac{c_p \frac{\partial \theta_v}{\partial z}\frac{\partial P^\kappa}{\partial z}}{(\frac{\partial u}{\partial z})^2 + (\frac{\partial v}{\partial z})^2}.$$

Negative values indicate unstable buoyancy and shear, small positive values (< 0.2) indicate dominantly unstable shear, and large positive values indicate dominantly stable stratification.

Turbulent eddy diffusion coefficients of momentum, heat and moisture in the surface layer, are calculated using stability-dependant functions based on Monin-Obukhov theory:

$$K_m(surface) = C_u \times u_* = C_D W_s$$

and

$$K_h(surface) = C_t \times u_* = C_H W_s$$

where $u_* = C_u W_s$ is the surface friction velocity, C_D is termed the surface drag coefficient, C_H the heat transfer coefficient, and W_s is the magnitude of the surface layer wind.

C_u is the dimensionless exchange coefficient for momentum from the surface layer similarity functions:

$$C_u = \frac{u_*}{W_s} = \frac{k}{\psi_m}$$

where k is the Von Karman constant and ψ_m is the surface layer non-dimensional wind shear given by

$$\psi_m = \int_{\zeta_0}^{\zeta} \frac{\phi_m}{\zeta} d\zeta.$$

Here ζ is the non-dimensional stability parameter, and ϕ_m is the similarity function of ζ which expresses the stability dependance of the momentum gradient. The functional form of ϕ_m is specified differently for stable and unstable layers.

C_t is the dimensionless exchange coefficient for heat and moisture from the surface layer similarity functions:

$$C_t = -\frac{(\overline{w'\theta'})}{u_* \Delta\theta} = -\frac{(\overline{w'q'})}{u_* \Delta q} = \frac{k}{(\psi_h + \psi_g)}$$

where ψ_h is the surface layer non-dimensional temperature gradient given by

$$\psi_h = \int_{\zeta_0}^{\zeta} \frac{\phi_h}{\zeta} d\zeta.$$

Here ϕ_h is the similarity function of ζ, which expresses the stability dependance of the temperature and moisture gradients, and is specified differently for stable and unstable layers according to Helfand and Schubert, 1995.

ψ_g is the non-dimensional temperature or moisture gradient in the viscous sublayer, which is the mostly laminar region between the surface and the tops of the roughness

elements, in which temperature and moisture gradients can be quite large. Based on Yaglom and Kader (1974):

$$\psi_g = \frac{0.55(Pr^{2/3} - 0.2)}{\nu^{1/2}}(h_0 u_* - h_{0_{ref}} u_{*_{ref}})^{1/2}$$

where Pr is the Prandtl number for air, ν is the molecular viscosity, z_0 is the surface roughness length, the subscript *ref* refers to a reference value, and $h_0 = 30 z_0$ with a maximum value over land of 0.01

For an unstable surface layer, the stability functions, chosen to interpolate between the condition of small values of β and the convective limit, are the KEYPS function (Panofsky, 1973) for momentum, and its generalization for heat and moisture:

$$\phi_m{}^4 - 18\zeta\phi_m{}^3 = 1 \qquad ; \qquad \phi_h{}^2 - 18\zeta\phi_h{}^3 = 1 \qquad .$$

The function for heat and moisture assures non-vanishing heat and moisture fluxes as the wind speed approaches zero.

For a stable surface layer, the stability functions are the observationally based functions of Clarke (1970), slightly modified for the momemtum flux:

$$\phi_m = \frac{1 + 5\zeta_1}{1 + 0.00794\zeta_1(1 + 5\zeta_1)} \qquad ; \qquad \phi_h = \frac{1 + 5\zeta_1}{1 + 0.00794\zeta(1 + 5\zeta_1)}.$$

where $\zeta_1 = min(\zeta, 1)$.

2.3 Coupling between the Turbulence Parameterization and MOSAIC

The influence of the heterogeneities of the land surface extends up to a level in the atmosphere defined as the 'blending height', which is a level within the planetary boundary layer above which the flow becomes horizontally homogeneous in the absence of other influences. Many studies using field measurements have determined that the blending height is variable, depending mostly on the nature of the surface roughness elements and ranging from 20 to 100 times the size of these elements (Brutsaert, 1997, and references therein).

The GEOS-Terra GCM extends the 'mosaic' approach upwards throughout the entire depth of the turbulent atmospheric boundary layer in an attempt to properly capture the vertical extent of the influence of the surface heterogeneity. There is, therefore, no level at which there is an explicit aggregation of the surface heterogeneities. Each individual 'tile' thereby retains its separate character up to the level that is dictated by the local turbulent kinetic energy. This is the closest approach to allowing the model to find its own 'model blending height', which is defined here as a level above which the flow over the different tiles begins to appear uniform.

The terms in the equations of motion that correspond to the vertical fluxes due to turbulence are computed for a GCM grid square at a GCM time. These terms are similar for all the atmospheric state variables (winds, temperature, moisture), and we present the moisture turbulent tendency as an illustration.

The grid-averaged tendency due to turbulent processes of the atmospheric specific humidity, q, at a grid square (i,j,k), is evaluated at time $t+\Delta t_{LSM}$ by:

$$\left(\frac{\partial q}{\partial t}_{i,j,k}\right)\Bigg|_{t+\Delta t_{LSM}} = -\left[\rho\frac{\partial\overline{w'q'}}{\partial z}\right]_{t+\Delta t_{LSM}} = \left[K\frac{\partial^2 q}{\partial z^2}\right]_{t+\Delta t_{LSM}} . \qquad (1)$$

where q' is the fluctuating component of q, ρ is the density of air, w' is the (turbulent) vertical component of the velocity field, t represents the GCM time, Δt_{LSM} is the time step of the evolution of the surface heat and moisture, and $[\,]$ represents a grid averaging operator, to be defined below. We have made use of the customary representation of the turbulent flux in terms of an eddy diffusion coefficient, K, and the gradient of the mean field. We evaluate the turbulent diffusion after the surface condition has evolved because the turbulent diffusion of heat and moisture near the surface affect and are affected by the surface and sub-surface heat balance, as calculated inside the Land Surface Model.

For every grid square and level, (we drop the grid point subindex noting that all expressions apply at an (i,j,k) point in the GCM domain) the moisture and temperature tendencies due to turbulent diffusion are functions of their surface values, namely, canopy vapor pressure, e_a, and the canopy temperature, T_c, which in turn, are functions of the time relative to the land surface processes. This is:

$$q = q(e_a, T_c) \quad \text{where} \quad e_a, T_c = e_a, T_c(t_{LSM})\,. \qquad (2)$$

A Taylor series expansion of equation (1) in the variable t, neglecting second and higher order terms, results in:

$$\frac{\partial q}{\partial t}\Bigg|_{t+\Delta t_{LSM}} = \left[K\frac{\partial^2}{\partial z^2}q(e_a,T_c)\Big|_t + \frac{\partial}{\partial t}\left(K\frac{\partial^2}{\partial z^2}q(e_a,T_c)\right)\Big|_t \Delta t_{LSM}\right] . \qquad (3)$$

In virtue of expression (2), using the chain rule in the right-hand side of equation (3) and defining

$$\delta e_a = \left(\frac{\partial}{\partial t}e_a\right)\Delta t_{LSM} \quad \text{and} \quad \delta T_c = \left(\frac{\partial}{\partial t}T_c\right)\Delta t_{LSM}\,, \qquad (4)$$

the expression for the turbulent tendency becomes:

$$\begin{aligned}\frac{\partial q}{\partial t}\Bigg|_{t+\Delta t_{LSM}} = & \left[K\frac{\partial^2}{\partial z^2}q(e_a,T_c)\Big|_t\right] \\ & + \left[K\frac{\partial}{\partial e_a}\left(\frac{\partial^2}{\partial z^2}q(e_a,T_c)\right)\Big|_t \delta e_a\right]\end{aligned} \qquad (5)$$

$$+\left[K\frac{\partial}{\partial T_c}\left(\frac{\partial^2}{\partial z^2}q(e_a,T_c)\right)\bigg|_t \delta T_c\right] ,$$

In the formulation of the MOSAIC LSM, e_a and T_c are computed for each tile in a grid square. In order to evaluate a grid-averaged turbulent tendency of humidity, and this is the essence of the MOSAIC implementation being addressed in this study, each of these equations is written for each tile in any grid square. The grid-averaged tendency is then determined by calculating the simple average over the tiles (weighted by their fractional areas) in a grid square. The influence of the surface heterogeneity, then, at any grid square, as represented by the differences in the characteristics of the turbulent layer above each tile, is propagated vertically by the turbulent diffusion. This is shown schematically in figure 2, where the individual character of the turbulent column above each tile is retained throughout the vertical domain of the GCM.

Each tile contained in a grid square has its own canopy temperature, T_c, but is placed underneath the same atmospheric column with a single temperature at each level, T_k. Each tile, therefore, is characterized by its own soil-to-air gradients of heat and moisture and hence its own measure of turbulent stability. Individual temporal tendencies of temperature and humidity, δT_c and δe_a are calculated. The evolution of the canopy temperature and vapor pressure at each tile is then used to calculate the turbulent fluxes at the surface, using equation 7, and the turbulent fluxes at the top edge of each GCM level k, using equation 5, resulting in a determination of

$$\frac{\partial q}{\partial t}^t + \Delta t_{LSM}{}_{turb} \tag{6}$$

for each tile. The calculation is performed for the column above each tile throughout the entire depth of the atmosphere, although it has significant impact only in the boundary layer. The divergence of the turbulent flux is then aggregated for each tile to provide a grid-averaged value at each level for use by the GCM's thermodynamic and moisture equations. In this way the GCM 'feels' the direct impact of the surface heterogeneity (tiles) throughout the depth of the boundary layer.

Fluxes of heat, moisture, and momentum at the land-surface interface calculated by the SVAT at the new surface skin temperature and humidity must be consistent with those calculated by the GCM surface layer scheme at the old skin temperature and humidity (Helfand and Schubert 1995).

As is done in Koster and Suarez, 1992b, each of the surface fluxes at the new temperatures and humidities can be written using a Taylor expansion and neglecting second and higher order terms:

$$\begin{aligned}
R_{lw}{}^{\uparrow} &= R_{lw}{}^{\uparrow}{}_t + \frac{dR_{lw}{}^{\uparrow}}{dT_c}{}_t \delta T_c \qquad (7)\\
H &= H_{old} + \frac{dH}{dT_c}{}_t \delta T_c + \frac{dH}{de_a}{}_t \delta e_a \\
E &= E_t + \frac{dE}{dT_c}{}_t \delta T_c + \frac{dE}{de_a}{}_t \delta e_a \\
G_D &= G_{Dt} + \frac{dG_D}{dT_c}{}_t \delta T_c
\end{aligned}$$

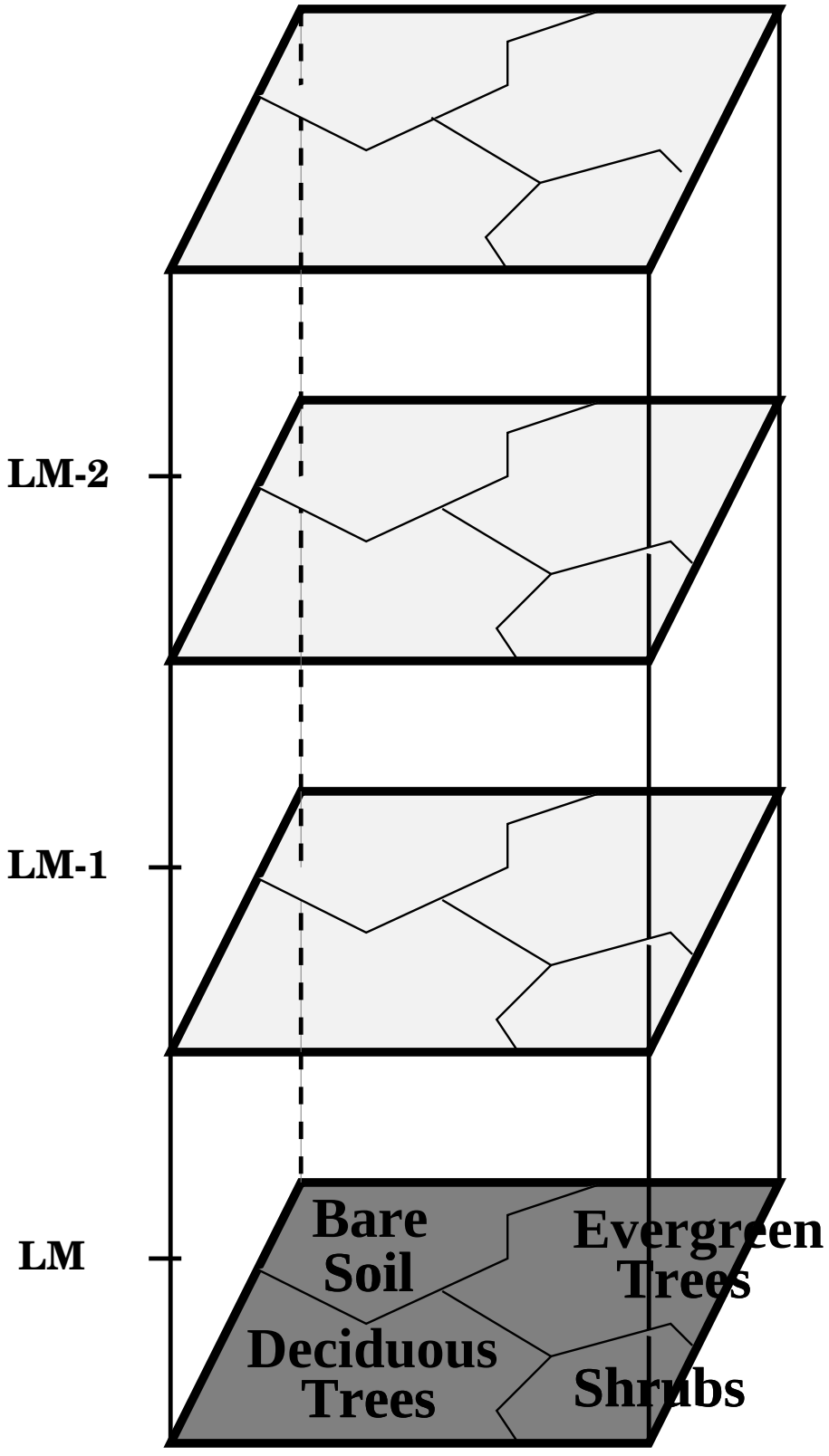

Figure 2: The Vertical Extent of MOSAIC tiles

GEOS-2 GCM Surface Type Designation

Type	Vegetation Designation
1	Broadleaf Evergreen Trees
2	Broadleaf Deciduous Trees
3	Needleleaf Trees
4	Ground Cover
5	Broadleaf Shrubs
6	Dwarf Trees (Tundra)
7	Bare Soil
8	Desert (Bright)
9	Glacier
10	Desert (Dark)
100	Ocean

Table 1: GEOS-2 GCM surface type designations used to compute surface roughness (over land) and surface albedo.

Finally, the surface energy budget and the equations that describe the evolution of the soil moisture can be solved at $t = t + \delta t_{LSM}$.

2.4 Surface Type Designation

The Koster-Suarez Land Surface Model (LSM) surface type classifications are shown in Table 1. The surface types and the percent of the grid cell occupied by any surface type were derived from the surface classification of Defries and Townshend (1994), and information about the location of permanent ice was obtained from the classifications of Dorman and Sellers (1989). The surface designation at 1°x1° resolution is shown in Figure 3. The determination of the land or sea category of surface type was made from NCAR's 10 minute by 10 minute Navy topography dataset, which includes information about the percentage of water-cover at any point. The data were averaged to the model's 4° x 5° and 2° x 2.5° grid resolutions, and any grid-box whose averaged water percentage was $\geq 60\%$ was defined as a water point. The 4° x 5° grid Land-Water designation was further modified subjectively to ensure sufficient representation from small but isolated land and water regions.

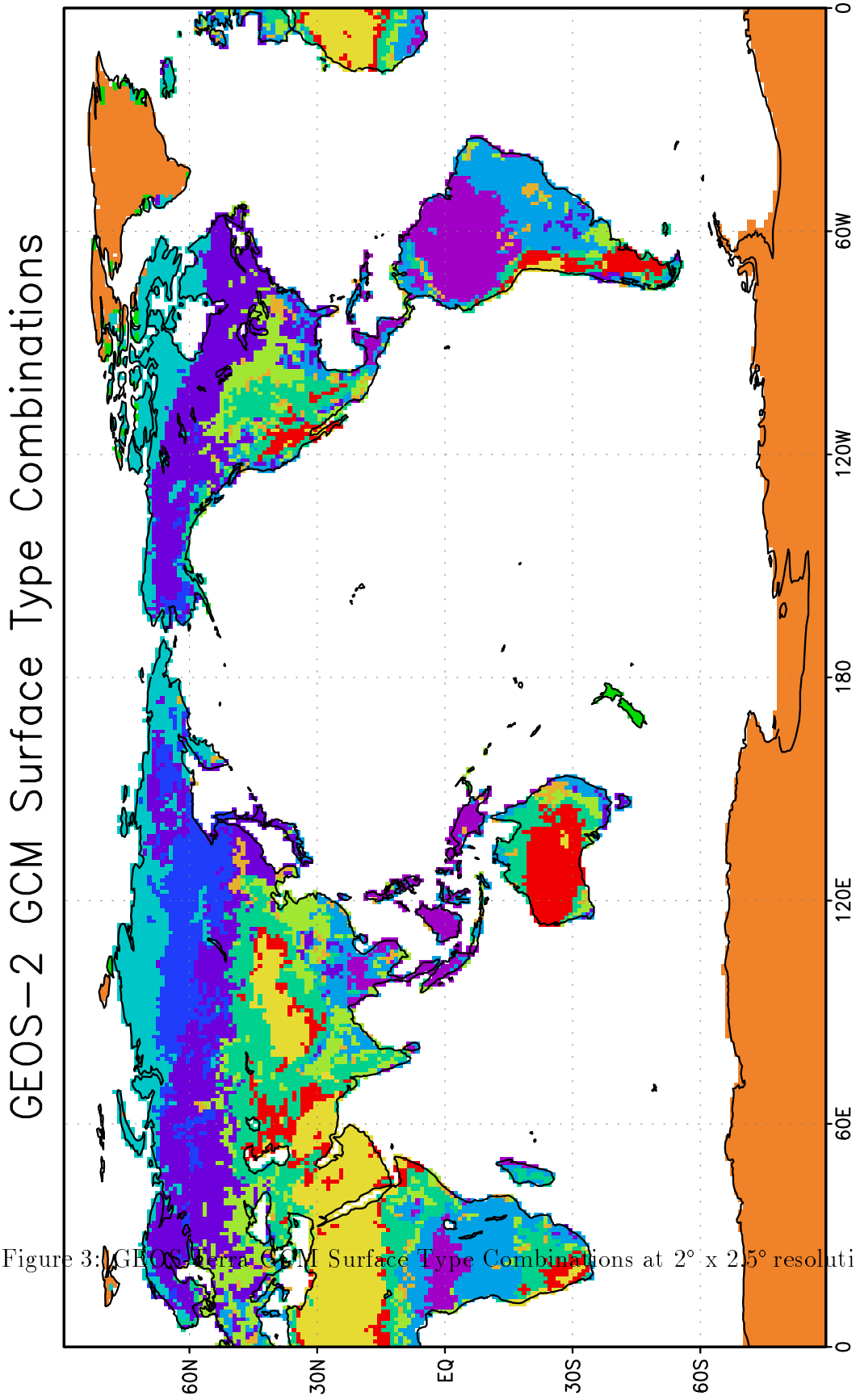

Figure 3: GEOS-Terra GCM Surface Type Combinations at 2° x 2.5° resolution.

Figure 4: Legend for figure 3

References

Betts, A. K., John H. Ball and Anton C. M. Beljaars, 1993: Comparison Between the Land Surface Response of the ECMWF Model and the FIFE-1987 Data. *Q. J. Roy. Meteor. Soc.*, **119**, 975-1001.

Bloom, S.C., L.L. Takacs, A.M. DaSilva, and D. Ledvina, 1996: Data Assimilation Using Incremental Analysis Updates. *Mon. Wea. Rev.*, **124**, 1256-1271.

Brutsaert, W.,1997. What on Earth is a 'Homogeneous Landsurface' in the Description of Heat and Water Vapor Fluxes? Could it be an Oxymoron?. *Water Res. Res.*

Chou, M.-D. and M.J. Suarez, 1994: An efficient thermal infrared radiation parameterization for use in general circulation models. NASA Technical Memorandum 104606 Volume 3, Goddard Space Flight Center, Greenbelt, MD 20771.

Gates, W. Lawrence, 1992: AMIP: The Atmospheric Model Intercomparison Project. *Bull. Am Met. Soc.*, **73**, 1962-1970

Helfand, H. M., M. and S. D. Schubert, 1995: Climatology of the Simulated Great Plains Low-Level Jet and Its contribution to the Continental Moisture Budget of the United States. *J. Climate*, **8**, 784-806.

Helfand, H. M., and J. C. Labraga, 1988: Design of a non-singular level 2.5 second-order closure model for the prediction of atmospheric turbulence. *J. Atmos. Sci.*, **45**, 113-132.

Pfaendtner, J., S. Bloom, D. Lamich, M. Seablom, M. Sienkiewicz, J. Stobie, and A. da Silva, 1995: Documentation of the Goddard Earth Observing System (GEOS) Data Assimilation System - Version 1, NASA Technical Memorandum 104606 Volume 4, Goddard Space Flight Center, Greenbelt, MD 20771, 58 pp.

Molod, A., Helfand, H. M., and L. L. Takacs, 1996: The Climatology of Parameterized Physical Processes in the GEOS-1 GCM and their Impact on the GEOS-1 Data Assimilation System. *J. Climate*, **9**, 764-785.

Moorthi, S., and M. J. Suarez, 1992: Relaxed Arakawa Schubert: A parameterization of moist convection for general circulation models. *Mon. Wea. Rev.*, **120**, 978-1002.

Schubert, S. D., and Y. Chang, 1996: An objective method for inferring sources of model error. *Mon.Wea.Rev.*, **124**, 325-340.

Schubert, S., C.-K. Park, Chung-Yu Wu, W. Higgins, Y. Kondratyeva, A. Molod, L. Takacs, M. Seablom, and R. Rood, 1995: A Multiyear Assimilation with the GEOS-1 System: Overview and Results. *NASA Tech. Memo. 104606*, Vol. **6.** Goddard Space Flight Center, Greenbelt, MD 20771.

Schubert, S.D., and R.B. Rood, 1995: Proceedings of the Workshop on the GEOS–1 five–year assimilation. NASA Tech. Memo. 104606, Vol. 7, 201 pp.

Schubert, S. D., J. Pfaendtner and R. Rood, 1993: An assimilated data set for Earth

Science applications. *Bull. Am Met. Soc.*, **74**, 2331-2342.

Sellers, P. J., Y. Mintz, Y. C. Sud and A. Dalcher, 1986: A Simple Biosphere Model (SiB) for Use within General Circulation Models. *J. Atmos. Sci.*, **43**, 505-531.

Suarez, M. J., and L. L. Takacs, 1995: Documentation of the Aries/GEOS Dynamical Core Version 2, NASA Technical Memorandum 104606 Volume 5, Goddard Space Flight Center, Greenbelt, MD 20771, 58 pp.

Sud, Y. C., and A. Molod, 1988: The roles of dry convection, cloud-radiation feedback processes and the influence of recent improvements in the parameterization of convection in the GLA GCM. *Mon. Wea. Rev.*, **116**, 2366-2387.

Takacs, L. L. , A. Molod, and T. Wang, 1994: Documentation of the Goddard Earth Observing System (GEOS) General Circulation Model-Version 1. NASA Technical Memorandum 104606 Volume 1, Goddard Space Flight Center, Greenbelt, MD 20771, 97 pp.

Takacs, L. L. and M.J. Suarez, 1996: Dynamical aspects of climate simulations using the GEOS General Circulation Model. NASA Technical Memorandum 104606 Volume 10, Goddard Space Flight Center, Greenbelt, MD 20771, 70 pp.

Zhou, J., Y.C. Sud, and K.-M. Lau, 1996: Impact of Orographically Induced Gravity Wave Drag in the GLA GCM, *Quart. J. Roy. Meteor. Soc.*, **122**, 903-927.